

# Development and application of a colloidal gold dual immunochromatography strip for detecting antibodies against African Swine Fever Virus

Shuai Zhang <sup>1,†</sup>, Yuzhu Zuo <sup>1,†,\*</sup>, Yan Li <sup>1</sup>, Jing Ma <sup>1</sup>, Chuanwen Wang <sup>1</sup>, Yunhuan Zhao <sup>1</sup>, Jinghui Fan<sup>1, 2, \*</sup>

<sup>1</sup>College of Veterinary Medicine, Hebei Agricultural University, Baoding 071001, China

<sup>2</sup>Hebei Veterinary Biotechnology Innovation Center, Baoding 071001, China

\*Corresponding author:

Jinghui Fan, Yuzhu Zuo

dyfjh@hebau.edu.cn, dyzyz@hebau.edu.cn.

†These authors contributed equally to this work

**Abstract:** African swine fever (ASF) virus (ASFV) is widely prevalent globally. Due to its rapid onset and the absence of effective vaccines or therapeutic drugs, ASFV has caused significant economic losses to the global pig industry. In recent years, the less pathogenic ASFV $\Delta$ CD2v strain with deleted or mutated EP402R gene has become gradually more prevalent. This prevalence has further increased the difficulty of ASFV control. Colloidal gold immunochromatographic strips (ICSs) allow rapid, sensitive, and low cost testing that does not rely on special equipment or skilled personnel, and are often used in on-site clinical testing. The rapid detection of pigs infected with ASFV helps prevent outbreaks of ASF. However, commercially available ICSs for on-site use only determine the presence or absence of ASFV antibodies. These strips cannot distinguish between ASFV  $\Delta$  CD2v and wild-type ASFV infections, which hinders the implementation of control strategies targeting different ASFV strains. To address these problems, we developed a double-target colloidal gold ICS with two detection lines for the detection of p30 and CD2v protein antibodies. The ICS employs colloidal gold as the tracer and p30 and CD2v proteins as the capture antigen. This dual ICS could specifically identify antibodies against p30 and CD2v proteins within 10 min without any equipment and no cross-reaction with positive antibodies against common swine disease pathogens. Compared with existing ICSs, the dual ICS exhibited significant advantages in differentiating ASFV $\Delta$ CD2v and wild-type ASFV infections. The test strips could detect serum antibodies diluted up to 1:1024 with high sensitivity. The novel ICS remained stable for 9 months at 4°C, 25°C and 37°C. Receiver operating characteristic curves demonstrated good test accuracy of the ICS (99.823% for p30 and CD2v proteins), compared with commercial ELISA kits. The findings indicate the promising potential of the novel ICS for rapid on-site detection of ASFV antibodies and differentiation of ASFV $\Delta$ CD2v and wild-type ASFV infections. The novel ICS could improve the effectiveness of ASFV control.

**Keywords:** ASFV; immunochromatographic strips; ASFV antibodies; differentiation

## 1. Introduction

African swine fever (ASF) is a highly pathogenic infectious disease that is caused by the ASF virus (ASFV)<sup>[1]</sup>. ASFV can infect domestic pigs and wild boars of all ages and is a serious threat to the pig industry worldwide<sup>[2]</sup>. ASF was first described in Kenya in 1921<sup>[3]</sup>, and has since spread to numerous regions globally. In 2018, China, the world's largest producer and consumer of pork, reported its initial case of ASFV infection<sup>[4]</sup>. Subsequently, ASF rapidly disseminated to all 31 provinces and cities across China, resulting in an estimated economic loss exceeding \$240 million<sup>[5]</sup>. In recent years, a less virulent natural ASFV in which the CD2v gene is deleted has emerged and become more prevalent. The mutant has caused chronic and persistent infections in pigs, creating new challenges to the prevention and control of ASF<sup>[6-9]</sup>. Currently, ASF is globally prevalent and remains inadequately controlled, imposing a substantial burden on the global pig industry<sup>[10]</sup>.

ASFV is the sole member of the Asfarviridae family. It is an enveloped DNA virus<sup>[11]</sup>. It is mainly composed of the genome, core shell, inner envelope, capsid, and external open reading frames (ORFs)<sup>[12]</sup>. The genome of ASFV spans approximately 170 to 190 kb and encodes more than 160 proteins<sup>[13]</sup>. Among them, p30 protein encoded by the CP204L gene is one of the most antigenic structural proteins involved in ASFV entry and infection<sup>[14, 15]</sup>. It is produced 2-4 h after infection with ASFV and is continuously expressed throughout infection<sup>[16]</sup>, which makes it an ideal target for ASF diagnosis. The p30 protein has been extensively utilized for the detection of early ASFV infections<sup>[17-19]</sup>. The CD2v protein is an outer-membrane glycosylated protein of wild-type ASFV with good immunogenicity and activity during the late stages of viral infection<sup>[20, 21]</sup>. It is encoded by EP402R, a virulence associated gene<sup>[22, 23]</sup>. Genetic changes in the EP402R gene due to mutations, insertions, or deletions led to the loss of expression and functional abolishment of the CD2v protein, and reduce the virulence of ASFV<sup>[5, 6, 8]</sup>. The highly immunogenic characteristics of CD2v make the protein a valuable component in the design and development of vaccines against ASFV as well as for antibody detection<sup>[5, 23-26]</sup>. The protein is also considered a critical target for the development of a diagnostic assay to distinguish the ASFV $\Delta$ CD2v strain from wild-type ASFV strains<sup>[5, 27-29]</sup>.

Currently, effective anti-ASFV agents and commercialized vaccines to prevent and control ASF are still not available, except in Vietnam where two attenuated vaccines have been licensed<sup>[12, 30-33]</sup>. Early diagnosis based on specific detection and timely elimination of the infected animals are essential for disease control. Given that pigs infected by attenuated mutants usually exhibit prolonged incubation, low-level and intermittent virus shedding, absence of viremia in the late stages of infection or after clinical recovery, accurate detection of ASFV-specific antibodies is more reliable for the identification of ASFV infected animals, especially animals infected with the less virulent mutants<sup>[6, 34]</sup>. Various types of serological diagnostic techniques for the detection of ASFV antibody have been used in the diagnosis of ASF. Among these techniques, enzyme linked immunosorbent assays (ELISAs) are most commonly used and recommended by the World Organisation for Animal Health<sup>[35]</sup>. Several ELISA methods have been developed based on highly antigenic viral proteins, which include p30, p17, pB602L, p22, p32, p54, p72, and CD2v<sup>[36-42]</sup>. These assays feature excellent sensitivity and specificity, and some can differentiate between ASFV  $\Delta$  CD2v and wild-type ASFV strains<sup>[5, 27-29]</sup>, offering a tool for ASFV serological diagnosis. However, ELISA requires trained technical personnel and specific instruments and equipment during the complex operation process. The approach is not suitable for rapid on-site detection<sup>[43, 44]</sup>.

The colloidal gold immunochromatographic assay (ICA) is a technique that is rapid, easy to perform, and inexpensive. ICA uses colloidal gold as a tracer. The specific antigen-antibody reactions yield a color that can be directly and visually observed within a few minutes. Special equipment and complicated handling procedures are not needed<sup>[45, 46]</sup>. These advantages made colloidal gold ICA a fast and convenient diagnostic method that is especially suitable for point-of-care detection. Commercial colloidal gold ICS and published colloidal gold ICA protocols enable the detection of ASFV antibodies<sup>[47-49]</sup>. However, there is no colloidal gold dual ICS for detecting antibodies to distinguish ASFV $\Delta$ CD2v and wild-type ASFV strains.

This study aimed to establish a colloidal gold dual ICS that can simultaneously detect antibodies against p30 and CD2v proteins. The study findings demonstrate that this ICS enables the early diagnosis of ASFV infections and effectively distinguishes the ASFV $\Delta$ CD2v and wild-type ASFV strains. The novel dual ICS has promising potential as technical support for controlling the spread and prevalence of ASF.

## **2. Materials and methods**

### **2.1 Sera**

Antibody-positive reference sera of wild-type ASFV strain (wild-type ASFV<sup>+</sup>) and ASFV $\Delta$ CD2v strain (ASFV<sup>+</sup> $\Delta$ CD2v), and antibody-negative reference sera of ASFV (ASFV<sup>-</sup>) were obtained from Qingdao Lijian Bio-tech Co. Ltd. (Qingdao, China). Antibody-positive sera of porcine reproductive and respiratory syndrome virus (PRRSV<sup>+</sup>), porcine pseudorabies virus (PRV<sup>+</sup>), porcine circovirus type 2 (PCV2<sup>+</sup>), and classical swine fever virus (CSFV<sup>+</sup>) were obtained from our laboratory collection. The status of these sera was verified by ELISA antibody detection kits (Putai Biology, Luoyang, China). Clinical serum samples (n = 566) were collected from pig farms suspected of ASFV infection in China (including Hebei, Henan, Shandong, and Jiangsu provinces).

### **2.2 Expression and purification of recombinant proteins ASFV-p30 and ASFV-CD2v**

The coding sequences of ASFV CP204L and EP402R genes were obtained from the NCBI database (ASFV Pig/HLJ/2018, GenBank: MK333180.1). The genes were treated with *EcoRI* and *BamHI*, and synthesized by Sangon Biotech (Sangon, Shanghai, China). The ASFV-p30 and ASFV-CD2v proteins were expressed, purified, and subjected to endotoxin removal following previously established protocols<sup>[29]</sup>. In brief, the recombinant proteins were obtained by ultrasonic disruption of isopropyl  $\beta$ -D-1-thiogalactoside (IPTG)-induced bacterial suspensions. The proteins were purified using a His-labeled protein purification kit (CWBI, Jiangsu, China) according to the kit instructions. The endotoxins in the purified proteins were removed and detected using a ToxinEraser Endotoxin Removal Kit (Genscript, Nanjing, China) and a ToxinSensor Chromogenic LAL Endotoxin Assay Kit (Genscript). The concentration and purity of the purified proteins were determined using a NanoDrop 2000 instrument (Thermo Fisher Scientific, Waltham, MA, USA). The purified ASFV-p30 and ASFV-CD2v proteins were analyzed using SDS-PAGE and Coomassie brilliant blue staining.

### **2.3 Western blotting**

The purified ASFV-p30 and ASFV-CD2v proteins were separated by SDS-PAGE and transferred to polyvinylidene fluoride (PVDF) membranes (Solarbio, Beijing, China). After being blocked with 5% skim milk powder in Tris buffered saline-Tween (TBST) at 37°C for 3 h, the PVDF membranes were incubated with antibody-positive reference sera of wild-type ASFV strain, ASFV $\Delta$ CD2v strain, and antibody-negative reference sera of ASFV as primary antibodies at 37°C for 3 h, respectively. After washing with TBST three times, the PVDF membranes were incubated with

horseradish peroxidase-conjugated rabbit anti-pig IgG(H+L) (Biodragon, Beijing, China) at 37°C for 1 h. Finally, eECL Western Blot Kit (CWBIO) and Odyssey Fc infrared imaging system (LICOR, Lincoln, NE, USA) were used to observe and analyze the results of Western blotting.

## **2.4 Preparation and identification of colloidal gold**

Colloidal gold solution was obtained by sodium citrate reduction. One milliliter of 1% chloroauric acid solution (HAuCl<sub>4</sub>; Jieyi, Shanghai, China) was added to 99 mL of boiling ultrapure water in a clear acid treated beaker on a magnetic stirrer. Then, 1.6 mL of 1% sodium citrate dihydrate (Solarbio) was added dropwise to the solution and heated continuously for 5 min until the color changed to red-purple. After being cooled to 25°C, the colloidal gold solution was filled to 100 mL with ultrapure water and stored away from light at 4°C. The quality of the colloidal gold was evaluated by spectroscopy scanning with an ultraviolet-visible (UV-VIS) spectrophotometer (JENWAY, Staffordshire, UK) and transmission electron microscopy (TEM) using a JEM-1400 instrument (JOEL, Akishima, Japan).

## **2.5 Optimization of preparation conditions for colloidal gold dual ICS**

### **2.5.1 Conjugation of staphylococcal protein A (SPA) with colloidal gold**

The pH values of colloidal gold solution were adjusted to 6, 6.5, 7, 7.5, 8, 8.5 and 9 by 0.2 mol/L K<sub>2</sub>CO<sub>3</sub>. Ten microliters of a 1 mg/mL solution of SPA (Prospec, East Brunswick, USA) was added to 200 uL colloidal gold solutions of the different pH values and conjugated at 4°C for 1 h. The colloidal gold solutions were centrifuged at 10,000 rpm for 30 min and resuspend. The optimal pH value of colloidal gold conjugated SPA was determined by measuring the absorbance by UV-VIS spectrophotometry (JENWAY) and visually observing the color change of colloidal gold. Different volumes of SPA (1 mg/mL) (5, 10, 15, 20, 25, 30, and 35 uL) were added to 200 uL colloidal gold solutions at the determined optimal pH value and conjugated at 4°C for 1 h. Then, 0.1 mL 10%(w/v) NaCl was added to each colloidal gold solution. The colloidal gold solutions were centrifuged at 10,000 rpm for 30 min and resuspended. The minimum concentration of colloidal gold conjugated SPA was determined by measuring the absorbance using the aforementioned UV-VIS spectrophotometer and visually observing the color change of colloidal gold. The optimal concentration of colloidal gold conjugated SPA was determined by adding a 20% volume of SPA to a minimum concentration of colloidal gold conjugated SPA. Under the optimal conditions, colloidal gold conjugated SPA was prepared following a previously reported method<sup>[50]</sup>. In brief, 1 mL SPA was slowly added to the colloidal gold solution and conjugated at 4°C for 1 h on a magnetic stirrer. Ten milliliters of 10% bovine serum albumin (BSA) was slowly added to the colloidal gold solution and stirred continuously for 30 min. The solution was centrifuged at 4°C at 10,000 rpm for 30 min. The red pellet was resuspended with 1/10 volume resolution buffer. The colloidal gold conjugated SPA was scanned using the aforementioned UV-VIS spectrophotometer.

### **2.5.2 Determination of optimal coating concentrations for Control line (C-line), Test 1 line (T1-line), and Test 2 line (T2-line)**

Monoclonal antibody to SPA (mAb-SPA; Bersee, Beijing, China), ASFV-p30, and ASFV-CD2v and were diluted to 0.5, 0.75, 1, 1.25, and 1.5 µg/µL with Tris-HCl (0.01 M, pH 7.5) and coated on the C, T1, and T2-line of the nitrocellulose (NC)membrane respectively. Antibody-positive reference sera of wild-type ASFV strain were detected by test strips. The optimal coating concentrations of ASFV-p30, ASFV-CD2v, and mAb-SPA were determined according to the color intensity of the C, T1, and T2-line of the NC membranes.

### **2.5.3 Determination of optimal sample dilution**



After determining the optimal coating concentrations of ASFV-p30, ASFV-CD2v, and mAb-SPA, antibody-positive reference serum of wild-type ASFV strain was diluted with sample diluent to 1:50, 1:100, 1:200, and 1:400. Each dilution of sera were detected using the test strips. The optimal sample dilution was determined based on the color intensity of T1, T2, and C-line of the NC membranes.

#### **2.5.4 Determination of optimal immunochromatographic time**

After determining the optimal coating concentrations of ASFV-p30, ASFV-CD2v, and mAb-SPA and sample dilution, antibody-positive reference serum of the wild-type ASFV strain was detected using the test strips. The results were observed at 5, 10, 15, 20, and 25 min following the detection of the antibody-positive reference serum sample. The optimal immunochromatography time was determined according to the color intensity of the T1, T2, and C-line of the NC membranes.

#### **2.6 Assembly of colloidal gold dual ICS**

The sample pad was blocked in the sample pad processing solution (0.01 M Tris-HCl, pH 7.5, 2.0% (w/v) BSA, 2.0% (w/v) sucrose, and 0.1% (w/v)  $\text{NaN}_3$ ) for 1 h. After removal, it was dried at 37°C for 2 h and stored at 4°C. The conjugated pad was blocked in the conjugated pad processing solution (0.01 M Tris-HCl, pH 7.5, 0.75% (w/v) trehalose, 0.5% (w/v) sucrose, 2% (w/v) BSA, and 0.5% (w/v) Triton X-100) for 3 h. After removal, it was dried at 37°C for 2 h. The colloidal gold conjugated SPA was added to the conjugate pad at 4°C for 1 h and dried at 37°C for 2 h. ASFV-p30, ASFV-CD2v, and mAb-SPA were coated on the NC membranes as the T1, T2, and C-line at 1  $\mu\text{L}/\text{cm}$ , respectively, and dried at 37°C for 1 h. The NC membrane and conjugate, sample, and absorbent pads were assembled in PVC base plate with an overlap of 2 mm. The assembled test strips were cut into 2.5 mm  $\times$  60 mm pieces, placed into plastic card slots, and stored in a sealed plastic bags containing desiccants at 4°C.

#### **2.7 Principle and result judgment of colloidal gold dual ICS**

One hundred microliters of the tested sera diluted 1:50 with sample diluent was added to the sample well of colloidal gold dual ICS and diffused forward through capillary action. The IgG in tested sera that reached the conjugated pad was bound by colloidal gold conjugated SPA and continued to diffuse forward. Upon diffusing to the T1-line (coated ASFV-p30) and T2-line (coated ASFV-CD2v), antibodies against p30 and CD2v proteins in the tested sera bound to ASFV-p30 (T1-line) and ASFV-CD2v (T2-line) proteins, resulting in visible red bands. Upon diffusing to the C-line (coated mAb-SPA), the colloidal gold conjugated SPA bound to mAb-SPA (C-line), resulting in a visible red band. Upon diffusing to the absorbent pad, the test was complete (Figure 1A).

One hundred microliters of the tested sera diluted 1:50 with sample diluent were individually added to the sample well of the colloidal gold dual ICS. The results were observed 10 min later. An antibody-positive serum of wild-type ASFV strain sample was recognized by the appearance of three visible red bands at the T1, T2, and C-lines. An antibody-positive serum of ASFV  $\Delta$ CD2v strain sample was recognized by the appearance of two visible red bands at the T1 and C-lines. An antibody-negative serum of ASFV sample was recognized by the appearance of only one visible red band at the C-line. The test was deemed invalid if there was no red band at the C-line (Figure 1B).

#### **2.8 Evaluation of colloidal gold dual ICS**

##### **2.8.1 Analytical specificity of colloidal gold dual ICS**

To evaluate the analytical specificity of the colloidal gold dual ICS prepared in this study,

antibody-positive sera of PRRSV, PRV, PCV2, and CSFV, antibody-positive reference sera of wild-type ASFV and ASFV  $\Delta$ CD2v strains, and antibody-negative reference sera of ASFV were detected by colloidal gold dual ICS.

### 2.8.2 Analytical sensitivity of colloidal gold dual ICS

To evaluate the analytical sensitivity of the colloidal gold dual ICS prepared in this study, antibody-positive reference sera of wild-type ASFV strain diluted from 1:128 to 1:4,096 in sample diluent were added to the sample well of colloidal gold dual ICS and detected.

### 2.8.3 Repeatability and reproducibility of colloidal gold dual ICS

To evaluate the repeatability of the colloidal gold dual ICS, five serum samples were detected by the same batch of colloidal gold dual ICS three times. The color intensity of the colloidal gold dual ICS were analyzed and the coefficient of variation (CV) (standard deviation [SD]/mean) was calculated. To evaluate the reproducibility of the colloidal gold dual ICS prepared in this study, five serum samples were detected by three batches of colloidal gold dual ICS in three laboratories. The color intensity of the colloidal gold dual ICS were analyzed and the CV was calculated.

### 2.8.4 Stability of colloidal gold dual ICS

To evaluate the stability of the colloidal gold dual ICS, antibody-positive reference sera of wild-type ASFV strain were detected by colloidal gold dual ICS stored at different temperatures (4, 25, and 37°C) and time periods (0, 3, 6, and 9 months). The color intensity of the colloidal gold dual ICS were analyzed and the CV was calculated.

### 2.8.5 Colloidal gold dual ICS examination of clinical serum samples

A total of 566 serum samples with suspected ASFV infection collected from different regions were detected by colloidal gold dual ICS, commercial ELISA kit based on p30 protein (JNT, Beijing, China), and commercial ELISA kit based on CD2v protein (Anheal Laboratories, Beijing, China). The applicability of colloidal gold dual ICS was evaluated in clinical samples by comparing them to the commercial ELISA kits.

## 2.9 Statistical analysis

All data were statistically analyzed using Origin 8.0 (OriginLab, Northampton, MA, USA) and SPSS 27.0 (IBM Corp, Armonk, NY, USA). The results of the analysis are expressed as the mean  $\pm$  SD.

## 3. Results

### 3.1 Expression and purification of ASFV-p30 and ASFV-CD2v recombinant proteins

Recombinant plasmids pET-32a-CP204L and pET-32a-EP402R were transformed into *Escherichia coli* BL21 (DE3) to express ASFV-p30 and ASFV-CD2v at the determined optimal induction conditions of 0.1 mM IPTG, 37°C, and 6 h. ASFV-p30 (36.2 kDa) and ASFV-CD2v (46.8 kDa) were resolved by SDS-PAGE (Figure 2). The recombinant proteins were purified by His-labeled protein purification kit according to the instructions. The endotoxin of the purified ASFV-p30 and ASFV-CD2v recombinant proteins were removed by ToxinEraser Endotoxin Removal Kit. The endotoxin content of purified recombinant proteins were  $< 0.01$  EU/mL by ToxinSensor Chromogenic LAL Endotoxin Assay Kit. The high concentration and purity of the ASFV-p30 and ASFV-CD2v proteins were demonstrated by SDS-PAGE and NanoDrop 2000 spectroscopy.

### 3.2 Western blotting

Western blotting was used to analyze the reactivity of recombinant proteins. The ASFV-p30 recombinant protein could react specifically with antibody-positive reference serum of wild-type ASFV and ASFV  $\Delta$ CD2v strains, recombinant protein ASFV-CD2v reacted specifically with

antibody-positive reference serum of wild-type ASFV strain, but not the ASFV  $\Delta$ CD2v strain (Figure 3). The findings indicate that the high reactivity of ASFV-p30 and ASFV-CD2v purified recombinant proteins.

### 3.3 Preparation and identification of colloidal gold

The prepared colloidal gold was wine red and transparent without precipitant or floating matter. UV-VIS spectrophotometry scan the colloidal gold at wavelengths ranging from 450-650 nm. The maximum absorption peak was at 520 nm and absorption peak width was narrow (500-550 nm), indicating that colloidal gold particles were relatively uniform (Figure 4A). TEM examination of the colloidal gold revealed uniformity of spherical shape and size distribution (Figure 4B). The findings demonstrated the uniformity and high quality of the prepared colloidal gold particles, with a morphology suitable for the development of the colloidal gold dual ICS.

### 3.4 Optimization of preparation conditions for colloidal gold dual ICS

#### 3.4.1 Conjugation of SPA with colloidal gold

The pH value of colloidal gold solutions was adjusted by adding different volumes of 0.2 mol/L  $K_2CO_3$  to determine the optimal pH value of colloidal gold conjugated SPA. When the pH was 7, the color of the colloidal gold solution was the same as that of the control group (Figure 5A). As well, the absorbance at 520 nm was highest (Figure 5B). Therefore, the optimal pH of colloidal gold conjugated SPA was 7.0. The optimal concentration of colloidal gold conjugated SPA was determined by adding different volumes of SPA (1 mg/mL) and 10% NaCl to colloidal gold solutions at the optimal pH. When  $\geq 20$   $\mu$ L SPA was added, the color of the colloidal gold solution was the same as that of the control group (Figure 5C). As well, the absorbance at 520 nm was highest (Figure 5D). Therefore, 0.107 mg/mL SPA was considered the optimal concentration of colloidal gold conjugated SPA.

UV-VIS spectroscopy was used to characterize colloidal gold conjugated with SPA. Compared to unconjugated colloidal gold, the colloidal gold conjugated SPA exhibited a maximum absorption peak at 525 nm, indicating successful conjugation (Figure 6).

#### 3.4.2 Determination of optimal coating concentrations for Control line (C-line), Test 1 line (T1-line), and Test 2 line (T2-line)

The optimal coating concentrations for the C, T1, and T2-line were determined by detecting the antibody-positive reference serum. When the mAb-SPA coated concentration of C-line was 0.75  $\mu$ g/ $\mu$ L, the ASFV-p30 coated concentration of T1-line was 1  $\mu$ g/ $\mu$ L and the ASFV-CD2v coated concentration of T2-line was 1  $\mu$ g/ $\mu$ L. The color intensities of the C, T1, and T2-line of the NC membranes were greatest and the red bands most clearly discerned with the naked eye (Figure 7). The coated concentrations of mAb-SPA (C-line), ASFV-p30 (T1-line), and ASFV-CD2v (T2-line) were determined to be 0.75, 1 and, 1  $\mu$ g/ $\mu$ L, respectively.

#### 3.4.3 Determination of optimal sample dilution

Antibody-positive reference serum of wild-type ASFV strain diluted 1:50, 1:100, 1:200, and 1:400 with sample diluent at were detected by test strips to determine the optimal sample dilution. When the antibody-positive reference serum of wild-type ASFV strain was diluted 1:50, the color intensities of the T1, T2, and C-line of NC membranes were greatest and the red bands were most clearly visible to the naked eye (Figure 8). Hence, 1:50 was considered the optimal sample dilution.

#### 3.4.4 Determination of optimal immunochromatographic time

The antibody-positive reference serum of the wild-type ASFV strain was detected using the test strips using different immunochromatography times of 5, 10, 15, 20, and 25 min to determine

the optimal immunochromatography time. With the increase of the immunochromatography time from 5 to 10 min, the color intensity of T1, T2, and C-line on NC membranes increased significantly. Further extension of the immunochromatography time to 15 min resulted in a gradual decrease in the color intensity of the T1 and T2-line (Figure 9). After comprehensively evaluating all factors, 10 min was considered the optimal immunochromatographic time.

### **3.5 Evaluation of colloidal gold dual ICS**

#### **3.5.1 Analytical specificity of colloidal gold dual ICS**

Antibody-positive sera of PRRSV, PRV, PCV2 and CSFV; antibody-positive reference sera of wild-type ASFV strain and ASFV  $\Delta$ CD2v strain; and antibody-negative reference sera of ASFV were used to evaluate the analytical specificity of colloidal gold dual ICS. Antibody-positive reference sera of wild-type ASFV strain produced three red bands on the T1, T2, and C-line. Antibody-positive reference sera of ASFV  $\Delta$ CD2v strain produced two red bands on the T1 and C-line. The other sera produced only a red band on the C-line. The colloidal gold dual ICS showed no cross-reactivity with other antibody-positive sera, indicating good analytical specificity (Figure 10).

#### **3.5.2 Analytical sensitivity of colloidal gold dual ICS**

Antibody-positive reference serum of wild-type ASFV strain diluted from 1:128 to 1:4,096 in sample diluent were assessed to evaluate the analytical sensitivity of the colloidal gold dual ICS strips. The colloidal gold dual ICS was capable of detecting antibody-positive serum diluted to 1:1,024, indicating good analytical sensitivity (Figure 11).

#### **3.5.3 Repeatability and reproducibility of colloidal gold dual ICS**

Five serum samples were detected in triplicate by the same batch of test strips to evaluate the repeatability of the colloidal gold dual ICS. The CV of color intensities of the C, T1, and T2-line were < 5%. Five serum samples were detected by three batches of test strips in three laboratories to evaluate the reproducibility of the colloidal gold dual ICS. The CV of color intensities of the C, T1, and T2-line were < 5% (Figure 12). The results demonstrated that the colloidal gold dual ICS exhibited excellent repeatability and reproducibility.

#### **3.5.4 Stability of colloidal gold dual ICS**

Antibody-positive reference sera of the wild-type ASFV strain were detected by test strips with different temperatures (4, 25, and 37°C) and time periods (0, 3, 6, and 9 months) to evaluate the stability of the colloidal gold dual ICS. The CV of color intensities of the test strips (C, T1, and T2-line) stored at the three temperatures and four time periods (0, 3, 6, and 9 months) were < 5% (Figure 13). The findings demonstrated the excellent stability of the colloidal gold dual ICS.

#### **3.5.5 Clinical serum samples detection of colloidal gold dual ICS**

A total of 566 serum samples obtained from animals with suspected ASFV infection were detected by test strips to evaluate the applicability of the colloidal gold dual ICS in clinical sample detection. The results of the colloidal gold dual ICS were compared with those of the commercial ELISA kits to calculate the test accuracy of the colloidal gold dual ICS. The colloidal gold dual ICS identified a total of 57 antibody-positive sera of ASFV (49 antibody-positive sera of wild-type ASFV strain, 8 antibody-positive sera of ASFV  $\Delta$ CD2v strain), and 509 antibody-negative sera of ASFV (Figure 14A, C). Commercial ELISA kit based on p30 protein were antibody-positive for produced 58 clinical serum samples and antibody-negative for samples (Figure 14A). Commercial ELISA kit based on CD2v protein produced anti-positive results for 50 clinical serum samples and antibody-negative results for 516 serum samples (Figure 14C). Only one antibody-positive sample on the T1 and T2-line showed a discrepancy. The test accuracies for both the T1-line (p30 protein)

and T2-line (CD2v protein) were 99.823% (Table 1). Based on these results, receiver operating characteristic (ROC) curves of p30 and CD2v proteins were constructed. The T1-line of the colloidal gold dual ICS demonstrated 100% sensitivity and 99.409% specificity relative to the commercial ELISA kit based on p30 protein, with an area under the curve (AUC) approaching 1 (Figure 14B). The T2-line of the colloidal gold dual ICS exhibited 100% sensitivity and 96.705% specificity relative to the commercial ELISA kit based on CD2v protein, with an AUC approaching 1 (Figure 14D). The kappa values were 0.990 and 0.989, respectively, indicating substantial agreement. The findings indicate an almost perfect concordance between the colloidal gold dual ICS and the commercial ELISA kits. The findings further suggest that the novel ICS is a reliable technical means for on-site diagnosis of ASFV antibodies and differentiation between the wild-type ASFV and ASFV $\Delta$ CD2v strains.

Table 1. Comparison of the results of the colloidal gold dual ICS with the commercial ELISA kits.

Methods and determination indices		The T1-line of the colloidal gold dual ICS		Total
		Positive	Negative	
The commercial ELISA kit based on p30 protein	Positive	57	1	58
	Negative	0	508	508
Total		57	509	566
Methods and determination indices		The T2-line of the colloidal gold dual ICS		Total
		Positive	Negative	
The commercial ELISA kit based on CD2v protein	Positive	49	1	50
	Negative	0	516	516
Total		49	517	566

## Discussion

ASFV has caused catastrophic damage to the global pig industry<sup>[2]</sup>. In the absence of commercial sources of effective vaccines and antiviral drugs, rapid and effective diagnostic methods are essential to identify ASFV infected pigs and track the spread of ASFV<sup>[51, 52]</sup>. PCR and fluorescent quantitative PCR methods for the detection of viral nucleic acid are important in the prevention and control of ASFV<sup>[53]</sup>. However, with the spread of ASFV globally, the less virulent ASFV $\Delta$ CD2v strain has emerged<sup>[6-8]</sup>. Pigs infected with ASFV $\Delta$ CD2v exhibited subacute and chronic clinical symptoms, and intermittent virus shedding. The detection rate of nucleic acid in surviving pigs or those with chronic infections in the non-shedding period of the infection gradually decreases after 42 days, but antibodies can persist for a long time<sup>[54]</sup>. Therefore, antibody detection is an essential part of ASF diagnosis. Establishing serological detection methods for the monitoring and diagnosis of ASFV infection is crucial for the effective prevention and control of ASFV. Various types of serological approaches for ASFV-specific antibodies detecting have been used in current ASF diagnosis. The commonly used in clinical applications include ELISA and colloidal gold ICA<sup>[44]</sup>, and numerous ELISA and colloidal gold ICA based on highly antigenic proteins, such as p30, p72, p54, and CD2v, have been widely developed<sup>[36-42, 47-49, 55]</sup>. Colloidal gold ICA is a rapid and

convenient detection method. The assay can be initiated by applying the analyte to the sample pad and does not require any additional reagents and processing steps. The reaction results can be directly observed by naked eyes and no instruments was required<sup>[56, 57]</sup>. Compared with ELISA, the colloidal gold ICA overcomes limitations that include such as relative complex time-consuming multistep procedure and requirements for trained personnel and specialized equipment, making it suitable for on-site clinical testing. Currently, commercial colloidal gold ICS, such as those from NBGen (Beijing, China) and Sinoreca-Biotech (Beijing, China), were widely used for clinical antibodies against ASFV detection. The published colloidal gold ICA also showed the practicality and high specificity and sensitivity for on-site detection. Zhu et al. described a double-antigen-sandwich lateral flow assay based on gold nanoparticle-conjugated ASFV major capsid protein p72<sup>[49]</sup>. The lateral flow assay could detect ASFV antibody in serum samples with high specificity in 10 min and detect clinically positive serum diluted up to 1:10,000 with high sensitivity. Wan et al. used a 1:1 gold-labeled p30 and p72 probe mixture as a gold-labeled antigen to develop a colloidal gold dual ICS for detecting ASFV antibodies<sup>[47]</sup>. The colloidal gold dual ICS could specifically detect ASFV antibodies within 5-10 min, achieving a maximum detection sensitivity in serum diluted 1:256. Geng et al. developed a colloidal gold ICS labeled with colloidal gold p72 trimers for the detection of antibodies against ASFV<sup>[48]</sup>. The test strip showed a higher sensitivity of detecting ASFV antibodies than a commercial ELISA kit. Liu et al. developed a high concentration labeled colloidal gold ICS for detecting ASFV p30 protein antibodies<sup>[55]</sup>. The coincidence rate between the developed colloidal gold ICS and ELISA was 93.5%. However, all of the forementioned ICS methods for detecting ASFV antibodies only determine the status of ASFV antibodies against ASFV, but do not distinguish the infections caused by wild-type ASFV or lower virulent ASFV  $\Delta$ CD2v strain. To meet the requirements, a quantum dot-based fluorescent ICA using CD2v as the diagnostic antigen to detect ASFV antibodies has been developed<sup>[58]</sup>. However, this ICA only uses CD2v protein as the detection antigen. When the detected result is negative, it is hard to determine whether the pig was not infected with ASFV or infected with CD2v-unexpressed mutational ASFV using this strip method alone. In addition, visualizing the assay results requires special equipment, thus the one-step detection advantage is lost in an application and the cost of the assay will increase. Therefore, the development of a rapid and convenient colloidal gold ICS for differential detection of wild-type ASFV strains and lower virulent ASFV  $\Delta$ CD2v strain on-site has become urgent.

Ideal candidates for developing sensitive and specific ASF serological diagnostic tests with better diagnostic performance, should be proteins with good antigenicity, strong specificity and early expression, or combinations of these attributes. Among the known functional proteins of ASFV, p30 protein is one of the most antigenic ASFV proteins. It is expressed in the early stages of viral infection and was continuously expressed throughout the infection<sup>[17-19]</sup>. Serological tests using p30 as antigen can basically be used for the whole process of monitoring after ASFV infection<sup>[38, 39]</sup>. The CD2v protein could stimulate the production of specific antibodies, and it was often used as a differential diagnostic indicator for the wild-type ASFV and lower virulent ASFV  $\Delta$ CD2v strains. Considering the advantages of colloidal gold ICA and the characteristics of p30 and CD2v proteins as antigens, in this study, p30 and CD2v proteins were selected as diagnosis antigens, and a rapid and accurate colloidal gold dual ICS for simultaneous detection and differentiation of specific antibodies against wild-type ASFV and lower virulent ASFV  $\Delta$ CD2v mutants was developed.

The quality of diagnosis antigens is particularly important for the accuracy of the developed

colloidal gold ICS. To ensure the practicality and reliability of colloidal gold dual ICS for on-site detection of antibodies against ASFV, development conditions were systematically optimized. Highly efficient expression of p30 and CD2v proteins was achieved in the *E. coli* prokaryotic expression system, and the high purity of p30 and CD2v proteins was verified by SDS-PAGE and NanoDrop 2000 spectroscopy. As well, the endotoxin was removed from the purified proteins to improve specificity and avoid false positive results due to endotoxin contamination in purified proteins. Furthermore, to improve the sensitivity of the colloidal gold dual ICS and ensure that the colloidal gold conjugate complex could better bind to p30 and CD2v proteins to form red bands, the purified proteins were fully dialyzed to remove urea and imidazole. Through these efforts, we successfully developed a convenient, accurate, sensitive, and specific colloidal gold dual ICS. The colloidal gold dual ICS could be observed the detection results quickly within 10 min after adding serum samples and effectively distinguish between the wild-type ASFV and lower virulent ASFV  $\Delta$ CD2v strains. The colloidal gold dual ICS did not cross-react with antibodies against common swine pathogens, effectively avoiding false positive results. The novel ICS system maintained high specificity while demonstrating high sensitivity, capable of detecting ASFV antibody-positive serum diluted up to 1024-fold. The sensitivity surpassed that of the colloidal gold dual ICS developed by Wan et al. for detecting ASFV p30 and p72 protein antibodies (1:256)<sup>[47]</sup> and the high concentration labeled colloidal gold ICS for ASFV p30 protein antibodies developed by Liu et al. (1:512)<sup>[55]</sup>. Repeatability, reproducibility, and stability were critical factors that influencing the field applications of colloidal gold dual ICS. In the of repeatability and reproducibility tests, the CV in the color intensities of the C, T1, and T2-line of NC membranes were consistently < 5%. Additionally, when testing serum samples using test strips stored at different temperatures (4, 25, and 37°C) and different time periods (0, 3, 6, and 9 months), the CV in the color intensities of the C, T1, and T2-line of NC membranes remained < 5%, indicating excellent repeatability, reproducibility, and stability. These characteristics ensured the reliability and credibility of the detection results. To evaluate the applicability of the developed colloidal gold dual ICS, 566 clinical serum samples were detected in parallel using commercial ELISA kits. Fifty-seven clinical serum samples were positive for antibodies against ASFV and 509 were negative. The ROC analysis showed the T1-line demonstrated a sensitivity of 100% and specificity of 99.409% relative to the commercial ELISA kit based on p30 protein. The T2-line demonstrated a sensitivity of 100% and specificity of 96.705% relative to the commercial ELISA kit based on CD2v protein. These performances were superior to those reported by Liu et al. (sensitivity of 90.9% and specificity of 96.2%)<sup>[55]</sup> and Zhu et al. (sensitivity of 98% and specificity of 97%)<sup>[49]</sup>. The test accuracies of the colloidal gold dual ICS for T1 and T2-line were both 99.823% (565/566), surpassing the concordance rates of the colloidal gold dual ICS developed by Wan et al. (98.8% for the Svanova ELISA kit and 98.6% for the Ingenasa ELISA kit)<sup>[41]</sup>, as well as those developed by Liu et al (93.5% for the ID.vet ELISA kit)<sup>[55]</sup> and Zhu et al. (97.8% for the Harbin Weike Biotechnology Co., Ltd. and ID vet. ELISA kit)<sup>[49]</sup>. Importantly, in the present study, among the 58 positive samples the colloidal gold dual ICS developed by the study successfully identified 8 ASFV  $\Delta$ CD2v strains. None of the existing conventional colloidal gold ICS can achieve this differential diagnosis. Therefore, the colloidal gold dual ICS facilitates on-site detection of ASFV antibodies in clinical settings and also effectively distinguishes between the wild-type ASFV and less virulent ASFV  $\Delta$ CD2v strains. Once the ASFV strain is identified, veterinarians can implement targeted measures based on the specific strain present in the pig farm, such as eliminating ASFV infected pigs, to

minimize ASFV-related losses.

In conclusion, a rapid and specific colloidal gold dual ICS based on p30 and CD2v was developed for distinguishing wild-type ASFV and ASFV- $\Delta$ CD2v infections. This approach is easy to perform and does not require specialized equipment or skilled personnel, and so is suitable for on-site detection. In addition, with continued research, an effective ASFV subunit vaccine based on CD2v protein may be developed in the future. The colloidal gold dual ICS can also be used to distinguish vaccinated pigs from naturally infected pigs, as well as detect the immunization effect of the vaccine. However, serum samples have currently only been collected from some provinces in China, rather than from different regions globally affected by ASFV. Therefore, before global promotion and application, serum samples from different countries and regions will be collected and the global universality of the colloidal gold dual ICS will be further evaluated.

#### Acknowledgments

This work was funded by Hebei Agriculture Research System (HBCT2024220201, HBCT2024220401), Science and Technology Program of Hebei Province (21326611D).

#### Conflicts of Interest

The authors declare that they have no known competing financial interests or personal relationships that could have appeared to influence the work reported in this paper.

#### Ethical statement

The experiments were undertaken following the principles and guidelines of the Ethics Committee of Hebei Agricultural University (the approval number: 2021069).

#### Availability of data and materials

The datasets generated during the current study are available from the corresponding author upon reasonable request.

#### Reference

- [1] Sánchez-Vizcaíno J M, Mur L, Gomez-Villamandos J C, *et al.* An update on the epidemiology and pathology of African swine fever[J]. *J Comp Pathol*, 2015, 152(1): 9-21.
- [2] Sánchez-Cordón P J, Montoya M, Reis A L, *et al.* African swine fever: A re-emerging viral disease threatening the global pig industry[J]. *Vet J*, 2018, 233: 41-48.
- [3] Montgomery R E. On a form of swine fever occurring in BritishEast Africa (Kenya Colony)[J]. *J Comp Pathol*, 1921, 34(159-191): 243-262.
- [4] Zhou X, Li N, Luo Y, *et al.* Emergence of African Swine Fever in China, 2018[J]. *Transbound Emerg Dis*, 2018, 65(6): 1482-1484.
- [5] Lv C, Zhao Y, Jiang L, *et al.* Development of a Dual ELISA for the Detection of CD2v-Unexpressed Lower-Virulence Mutational ASFV[J]. *Life (Basel)*, 2021, 11(11): 1214.
- [6] Sun E, Zhang Z, Wang Z, *et al.* Emergence and prevalence of naturally occurring lower virulent African swine fever viruses in domestic pigs in China in 2020[J]. *Sci China Life Sci*, 2021, 64(5): 752-765.
- [7] Zhao K, Shi K, Zhou Q, *et al.* The Development of a Multiplex Real-Time Quantitative PCR Assay



- for the Differential Detection of the Wild-Type Strain and the MGF505-2R, EP402R and I177L Gene-Deleted Strain of the African Swine Fever Virus[J]. *Animals (Basel)*, 2022, 12(14): 1754.
- [8] Gallardo C, Soler A, Rodze I, *et al.* Attenuated and non-haemadsorbing (non-HAD) genotype II African swine fever virus (ASFV) isolated in Europe, Latvia 2017[J]. *Transbound Emerg Dis*, 2019, 66(3): 1399-1404.
- [9] Shi K, Liu H, Yin Y, *et al.* Molecular Characterization of African Swine Fever Virus From 2019-2020 Outbreaks in Guangxi Province, Southern China[J]. *Front Vet Sci*, 2022, 9: 912224.
- [10] Kedkovid R, Sirisereewan C, Thanawongnuwech R. Major swine viral diseases: an Asian perspective after the African swine fever introduction[J]. *Porcine Health Manag*, 2020, 6: 20.
- [11] Li Z, Chen W, Qiu Z, *et al.* African Swine Fever Virus: A Review[J]. *Life (Basel)*, 2022, 12(8): 1225.
- [12] Revilla Y, Pérez-Núñez D, Richt J A. African Swine Fever Virus Biology and Vaccine Approaches[J]. *Adv Virus Res*, 2018, 100: 41-74.
- [13] de Villiers E P, Gallardo C, Arias M, *et al.* Phylogenomic analysis of 11 complete African swine fever virus genome sequences[J]. *Virology*, 2010, 400(1): 128-136.
- [14] Hübner A, Petersen B, Keil G M, *et al.* Efficient inhibition of African swine fever virus replication by CRISPR/Cas9 targeting of the viral p30 gene (CP204L)[J]. *Sci Rep*, 2018, 8(1): 1449.
- [15] Jia N, Ou Y, Pejsak Z, *et al.* Roles of African Swine Fever Virus Structural Proteins in Viral Infection[J]. *J Vet Res*, 2017, 61(2): 135-143.
- [16] Lithgow P, Takamatsu H, Werling D, *et al.* Correlation of cell surface marker expression with African swine fever virus infection[J]. *Vet Microbiol*, 2014, 168(2-4): 413-419.
- [17] Cubillos C, Gómez-Sebastian S, Moreno N, *et al.* African swine fever virus serodiagnosis: a general review with a focus on the analyses of African serum samples[J]. *Virus Res*, 2013, 173(1): 159-167.
- [18] Argilaguet J M, Pérez-Martín E, Nofrías M, *et al.* DNA vaccination partially protects against African swine fever virus lethal challenge in the absence of antibodies[J]. *PLoS One*, 2012, 7(9): e40942.
- [19] Lacasta A, Ballester M, Monteagudo P L, *et al.* Expression library immunization can confer protection against lethal challenge with African swine fever virus[J]. *J Virol*, 2014, 88(22): 13322-13332.
- [20] Dixon L K, Abrams C C, Bowick G, *et al.* African swine fever virus proteins involved in evading host defence systems[J]. *Vet Immunol Immunopathol*, 2004, 100(3-4): 117-134.
- [21] Borca M V, Kutish G F, Afonso C L, *et al.* An African swine fever virus gene with similarity to the T-lymphocyte surface antigen CD2 mediates hemadsorption[J]. *Virology*, 1994, 199(2): 463-468.
- [22] Chen W, Zhao D, He X, *et al.* A seven-gene-deleted African swine fever virus is safe and effective as a live attenuated vaccine in pigs[J]. *Sci China Life Sci*, 2020, 63(5): 623-634.
- [23] Monteagudo P L, Lacasta A, López E, *et al.* BA71ΔCD2: a New Recombinant Live Attenuated African Swine Fever Virus with Cross-Protective Capabilities[J]. *J Virol*, 2017, 91(21): e01058-01017.
- [24] Teklue T, Wang T, Luo Y, *et al.* Generation and Evaluation of an African Swine Fever Virus Mutant with Deletion of the CD2v and UK Genes[J]. *Vaccines (Basel)*, 2020, 8(4): 763.
- [25] Song J, Wang M, Zhou L, *et al.* A candidate nanoparticle vaccine comprised of multiple epitopes of the African swine fever virus elicits a robust immune response[J]. *J Nanobiotechnology*, 2023, 21(1): 424.
- [26] Feng Z, Chen J, Liang W, *et al.* The recombinant pseudorabies virus expressing African swine fever

- virus CD2v protein is safe and effective in mice[J]. *Virol J*, 2020, 17(1): 180.
- [27] Jiang W, Jiang D, Li L, *et al*. Development of an indirect ELISA for the identification of African swine fever virus wild-type strains and CD2v-deleted strains[J]. *Front Vet Sci*, 2022, 9: 1006895.
- [28] Wang L, Fu D, Tesfagaber W, *et al*. Development of an ELISA Method to Differentiate Animals Infected with Wild-Type African Swine Fever Viruses and Attenuated HLJ/18-7GD Vaccine Candidate[J]. *Viruses*, 2022, 14(8): 1731.
- [29] Zhang S, Zuo Y, Gu W, *et al*. A triple protein-based ELISA for differential detection of ASFV antibodies[J]. *Front Vet Sci*, 2024, 11: 1489483.
- [30] Borca M V, Ramirez-Medina E, Silva E, *et al*. Development of a Highly Effective African Swine Fever Virus Vaccine by Deletion of the I177L Gene Results in Sterile Immunity against the Current Epidemic Eurasia Strain[J]. *J Virol*, 2020, 94(7): e02017-02019.
- [31] Gladue D P, Ramirez-Medina E, Vuono E, *et al*. Deletion of the A137R Gene from the Pandemic Strain of African Swine Fever Virus Attenuates the Strain and Offers Protection against the Virulent Pandemic Virus[J]. *J Virol*, 2021, 95(21): e0113921.
- [32] Pérez-Núñez D, Sunwoo S Y, García-Belmonte R, *et al*. Recombinant African Swine Fever Virus Arm/07/CBM/c2 Lacking CD2v and A238L Is Attenuated and Protects Pigs against Virulent Korean Paju Strain[J]. *Vaccines (Basel)*, 2022, 10(12): 1992.
- [33] Tran X H, Le T T P, Nguyen Q H, *et al*. African swine fever virus vaccine candidate ASFV-G-ΔI177L efficiently protects European and native pig breeds against circulating Vietnamese field strain[J]. *Transbound Emerg Dis*, 2022, 69(4): e497-e504.
- [34] Gallardo C, Soler A, Nurmoja I, *et al*. Dynamics of African swine fever virus (ASFV) infection in domestic pigs infected with virulent, moderate virulent and attenuated genotype II ASFV European isolates[J]. *Transbound Emerg Dis*, 2021, 68(5): 2826-2841.
- [35] WOA. World Organisation for Animals Health. Terrestrial Manual Chapter 3.8.1: African swine fever (Infection with African swine fever virus). [https://www.oie.int/fileadmin/Home/eng/Health\\_standards/tahm/3.08.01](https://www.oie.int/fileadmin/Home/eng/Health_standards/tahm/3.08.01).
- [36] Li D, Zhang Q, Liu Y, *et al*. Indirect ELISA Using Multi-Antigenic Dominants of p30, p54 and p72 Recombinant Proteins to Detect Antibodies against African Swine Fever Virus in Pigs[J]. *Viruses*, 2022, 14(12): 2660.
- [37] Li L, Qiao S, Li G, *et al*. The Indirect ELISA and Monoclonal Antibody against African Swine Fever Virus p17 Revealed Efficient Detection and Application Prospects[J]. *Viruses*, 2022, 15(1): 50.
- [38] Giménez-Lirola L G, Mur L, Rivera B, *et al*. Detection of African Swine Fever Virus Antibodies in Serum and Oral Fluid Specimens Using a Recombinant Protein 30 (p30) Dual Matrix Indirect ELISA[J]. *PLoS One*, 2016, 11(9): e0161230.
- [39] Zhou L, Song J, Wang M, *et al*. Establishment of a Dual-Antigen Indirect ELISA Based on p30 and pB602L to Detect Antibodies against African Swine Fever Virus[J]. *Viruses*, 2023, 15(9): 1845.
- [40] Nah J J, Kwon O K, Choi J D, *et al*. Development of an indirect ELISA against African swine fever virus using two recombinant antigens, partial p22 and p30[J]. *J Virol Methods*, 2022, 309: 114611.
- [41] Li J, Jiao J, Liu N, *et al*. Novel p22 and p30 dual-proteins combination based indirect ELISA for detecting antibodies against African swine fever virus[J]. *Front Vet Sci*, 2023, 10: 1093440.
- [42] Jung M C, Le V P, Yoon S W, *et al*. A Robust Quadruple Protein-Based Indirect ELISA for Detection of Antibodies to African Swine Fever Virus in Pigs[J]. *Microorganisms*, 2023, 11(11): 2758.

- [43] Bergeron H C, Glas P S, Schumann K R. Diagnostic specificity of the African swine fever virus antibody detection enzyme-linked immunosorbent assay in feral and domestic pigs in the United States[J]. *Transbound Emerg Dis*, 2017, 64(6): 1665-1668.
- [44] Zhang X, Zhou L, Ge X, *et al*. Advances in the diagnostic techniques of African swine fever[J]. *Virology*, 2025, 603: 110351.
- [45] Vilela D, González M C, Escarpa A. Sensing colorimetric approaches based on gold and silver nanoparticles aggregation: chemical creativity behind the assay. A review[J]. *Anal Chim Acta*, 2012, 751: 24-43.
- [46] Zhou G, Mao X, Juncker D. Immunochromatographic assay on thread[J]. *Anal Chem*, 2012, 84(18): 7736-7743.
- [47] Wan Y, Shi Z, Peng G, *et al*. Development and application of a colloidal-gold dual immunochromatography strip for detecting African swine fever virus antibodies[J]. *Appl Microbiol Biotechnol*, 2022, 106(2): 799-810.
- [48] Geng R, Sun Y, Li R, *et al*. Development of a p72 trimer-based colloidal gold strip for detection of antibodies against African swine fever virus[J]. *Appl Microbiol Biotechnol*, 2022, 106(7): 2703-2714.
- [49] Zhu W, Meng K, Zhang Y, *et al*. Lateral Flow Assay for the Detection of African Swine Fever Virus Antibodies Using Gold Nanoparticle-Labeled Acid-Treated p72[J]. *Front Chem*, 2021, 9: 804981.
- [50] Yu X, Jiang Y, Zhang S, *et al*. Development of a colloidal gold immunochromatographic strip with enhanced signal for the detection of bovine parvovirus[J]. *Front Microbiol*, 2023, 14: 1174737.
- [51] Sánchez E G, Pérez-Núñez D, Revilla Y. Development of vaccines against African swine fever virus[J]. *Virus Res*, 2019, 265: 150-155.
- [52] Teklue T, Sun Y, Abid M, *et al*. Current status and evolving approaches to African swine fever vaccine development[J]. *Transbound Emerg Dis*, 2020, 67(2): 529-542.
- [53] Zhang X, Liu X, Wu X, *et al*. A colloidal gold test strip assay for the detection of African swine fever virus based on two monoclonal antibodies against P30[J]. *Arch Virol*, 2021, 166(3): 871-879.
- [54] Petrov A, Forth J H, Zani L, *et al*. No evidence for long-term carrier status of pigs after African swine fever virus infection[J]. *Transbound Emerg Dis*, 2018, 65(5): 1318-1328.
- [55] Liu H C, Liu R C, Hu M R, *et al*. Development of high-concentration labeled colloidal gold immunochromatographic test strips for detecting african swine fever virus p30 protein antibodies[J]. *Heliyon*, 2024, 10(3): e25214.
- [56] Khlebtsov B, Khlebtsov N. Surface-Enhanced Raman Scattering-Based Lateral-Flow Immunoassay[J]. *Nanomaterials (Basel)*, 2020, 10(11): 2228.
- [57] Dykman L, Khlebtsov N. Gold nanoparticles in biomedical applications: recent advances and perspectives[J]. *Chem Soc Rev*, 2012, 41(6): 2256-2282.
- [58] Niu Y, Zhang G, Zhou J, *et al*. Differential diagnosis of the infection caused by wild-type or CD2v-deleted ASFV strains by quantum dots-based immunochromatographic assay[J]. *Lett Appl Microbiol*, 2022, 74(6): 1001-1007.

Figure 1. Schematic interpretation and result judgment of the colloidal gold dual ICS. (A). Schematic interpretation of the colloidal gold dual ICS. (B). Result judgment of the colloidal gold dual ICS.

Figure 2. SDS-PAGE analysis of ASFV-p30 and ASFV-CD2v proteins. (A, B). ASFV-p30 (A) and ASFV-CD2v protein (B) were analyzed by SDS-PAGE. M: Protein marker; 1: Before induction; 2: After induction; 3: Results of proteins purification.

Figure 3. Western blotting analysis of ASFV-p30 and ASFV-CD2v proteins. (A-C). Antibody-positive reference serum of wild-type ASFV strain (A), ASFV  $\Delta$ CD2v strain (B), and antibody-negative reference sera of ASFV (C) were used as the as primary antibodies. M: Protein marker; 1: ASFV-p30 protein; 2: ASFV-CD2v protein.

Figure 4. Characterization of colloidal gold by UV-VIS spectrophotometry (A) and TEM (B).

Figure 5. Determination of the optimal pH value and concentration of colloidal gold conjugated SPA. (A) Colors of colloidal gold solutions with different pH values. Samples 1-7 have pH values of 6, 6.5, 7, 7.5, 8, 8.5, and 9, respectively. Vial 8 is the Control. (B). The absorbance (520 nm) of colloidal gold solution with different pH values. (C). Determination of the optimal concentration of colloidal gold conjugated SPA. (A). The color of the colloidal gold solution with different volumes of SPA. Vials 1-7 contain 5, 10, 15, 20, 25, 30, and 35  $\mu$ L, respectively. Vial 8 is the Control. (D). Absorbance at 520 nm of colloidal gold solutions with the different volumes of SPA.

Figure 6. UV-VIS spectrophotometry plots of colloidal gold (A) and colloidal gold conjugated SPA (B).

Figure 7. Determination of optimal coating concentrations for the C, T1, and T2-line. (A). The detection of optimal coating concentrations by colloidal gold dual ICS. (B). The color intensities of the C, T1, and T2-line of NC membranes with different coating concentrations.

Figure 8. Determination of optimal sample dilution. (A). The detection of optimal sample dilution by colloidal gold dual ICS. (B). The color intensities of the C, T1, and T2-line of NC membranes with different sample dilutions.

Figure 9. Determination of optimal immunochromatographic time. (A). The detection of optimal immunochromatographic time by colloidal gold dual ICS. (B). The color intensities of C, T1, and T2-line of NC membranes with different immunochromatographic times.

Figure 10. Analytical specificity of the colloidal gold dual ICS. (A). The analytical specificity of colloidal gold dual ICS. (B). The color intensities of the C, T1, and T2-line of NC membranes with different sera.

Figure 11. Analytical sensitivity of the colloidal gold dual ICS. (A). The analytical sensitivity of colloidal gold dual ICS. (B). The color intensities of C, T1, and T2-line of NC membranes with different serum dilutions.

Figure 12. Repeatability and reproducibility of the colloidal gold dual ICS. (A). The mean  $\pm$  SD of color intensities of the C, T1, and T2-line of five serum samples tested in triplicate using the test strips. (B). The mean  $\pm$  SD of color intensities of the C, T1, and T2-line of five serum samples tested using the test strips in three laboratories.

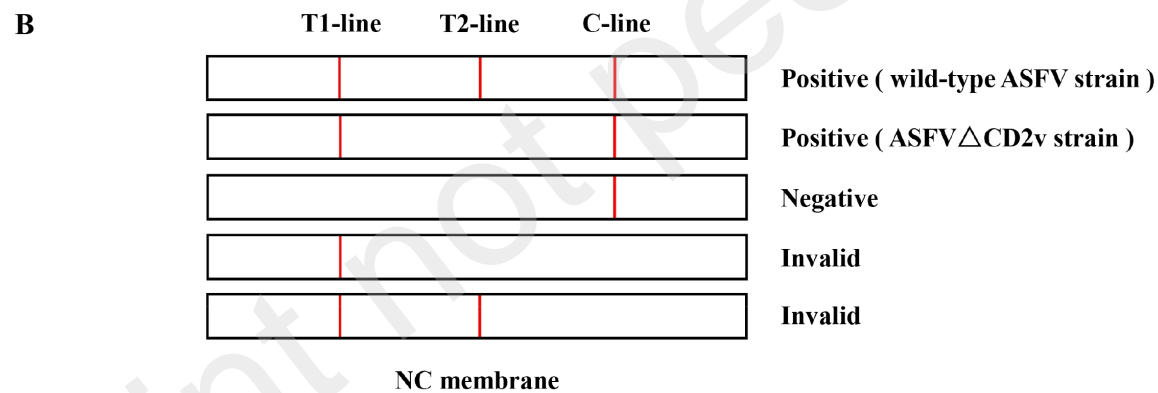
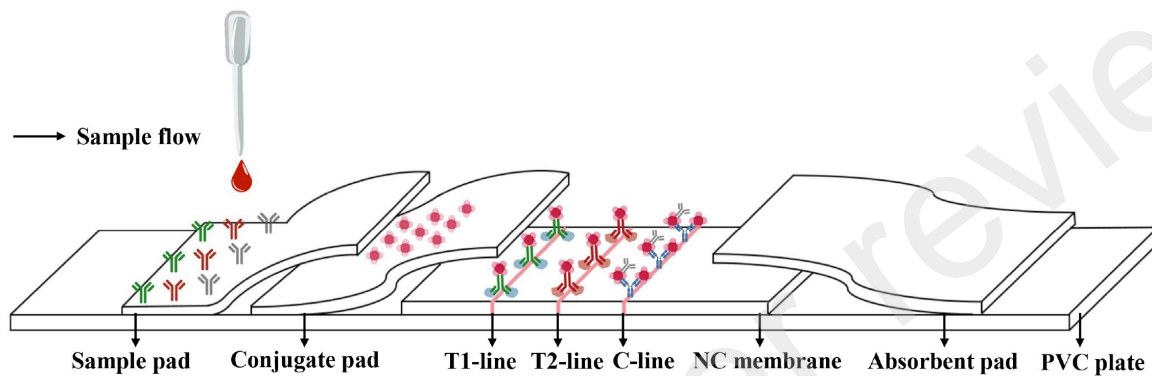
Figure 13. Stability of the colloidal gold dual ICS. The mean  $\pm$  SD of color intensities of the C, T1, and T2-line of five reference sera assessed by test strips at 0, 3, 6, and 9 months at 4°C (A), 25°C (B), and 37°C (C).

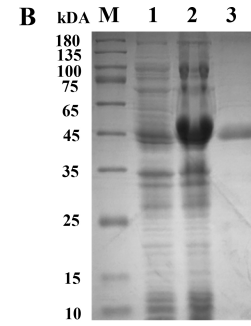
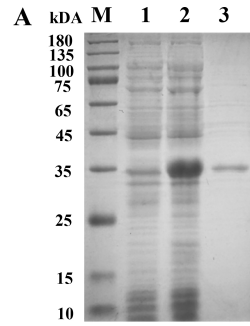
Figure 14. Applicability evaluation of the colloidal gold dual ICS in clinical samples. The results (A) and ROC analysis (B) of the colloidal gold dual ICS (T1-line) and the commercial ELISA kit

680 (p30 protein). The results (C) and ROC analysis (D) of the colloidal gold dual ICS (T2-line) and the  
681 commercialized ELISA kit (CD2v protein).  
682

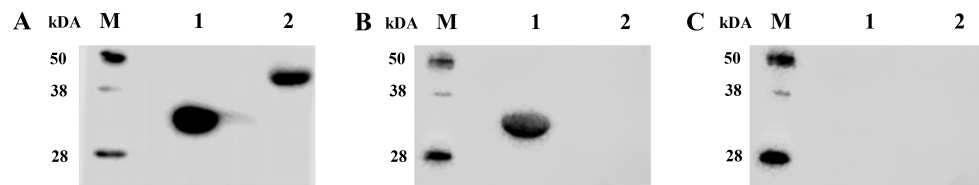
Preprint not peer reviewed

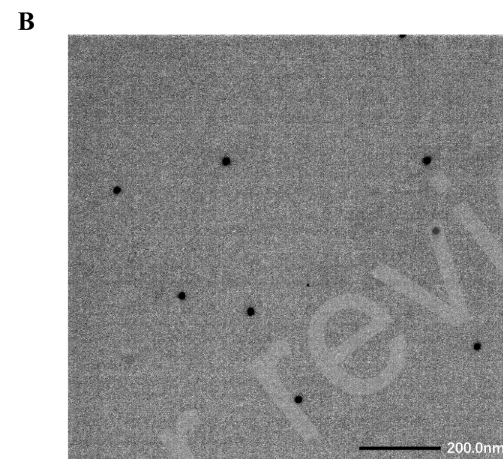
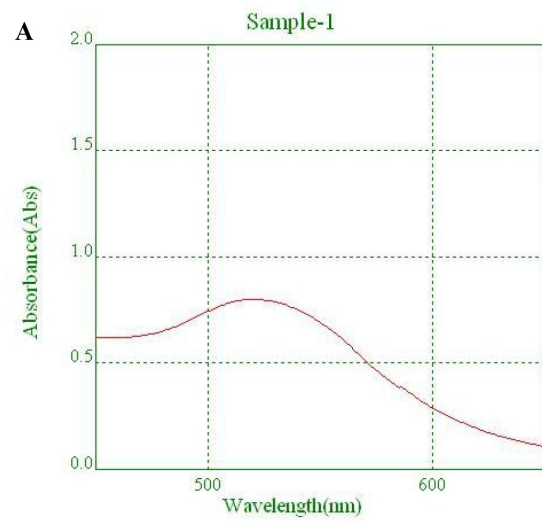
- A**
- Antibody against p30 protein
  - Antibody against CD2v protein
  - Non-specific antibodies
  - Colloidal gold conjugated SPA
  - p30 protein
  - CD2v protein
  - Mab-SPA

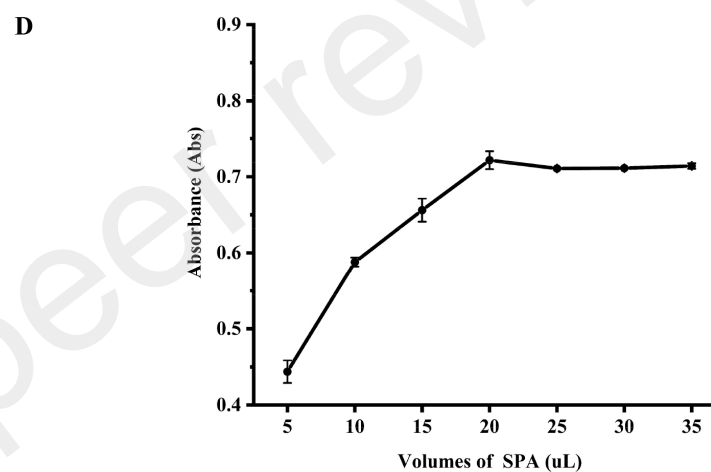
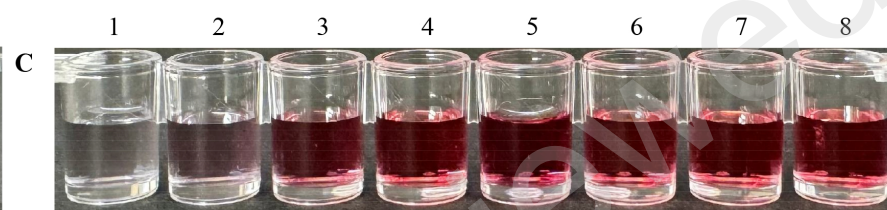
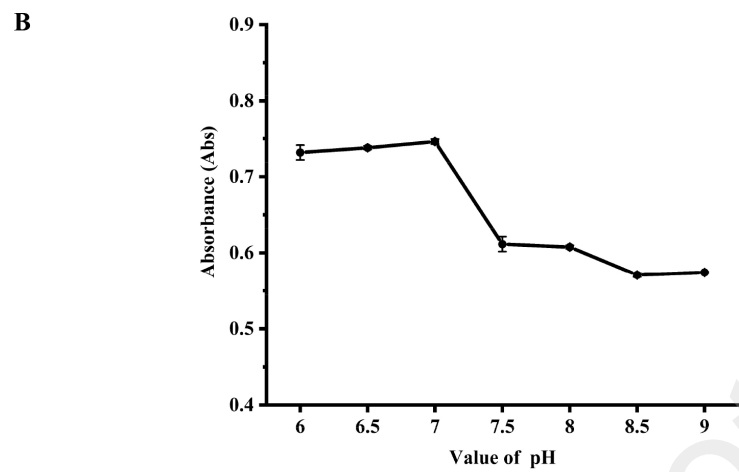
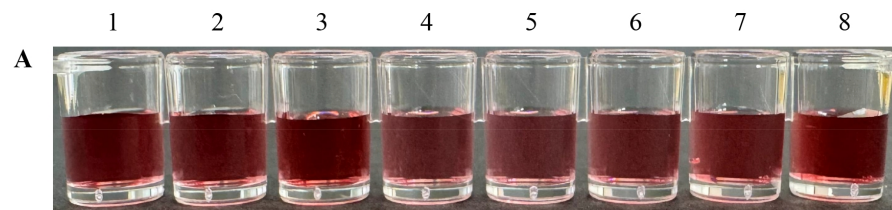


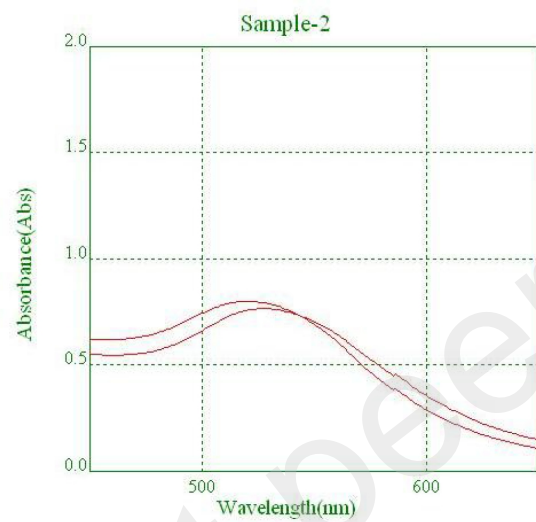




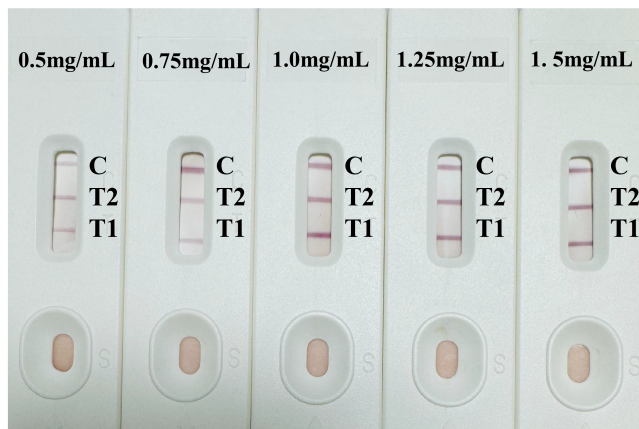




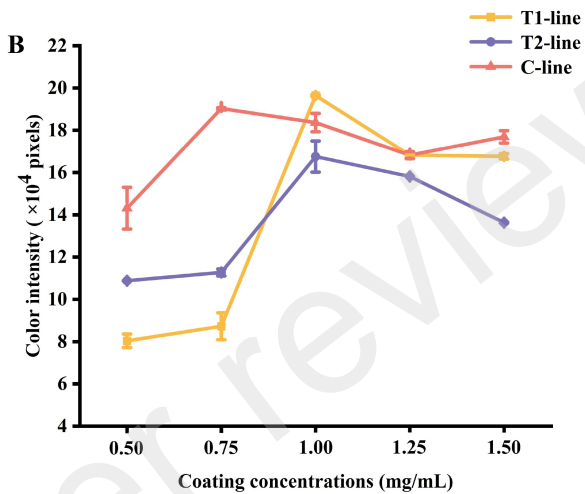


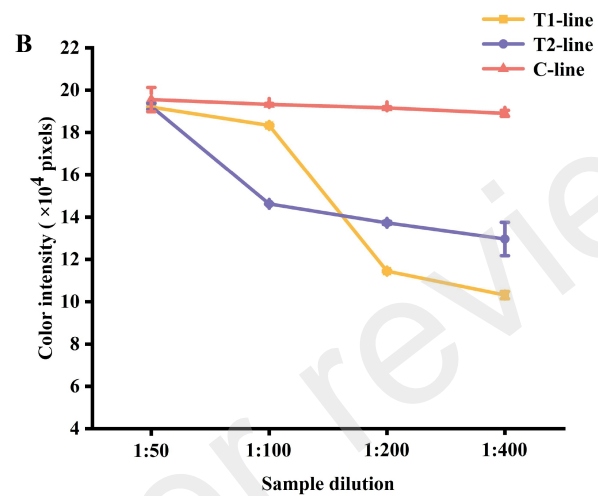
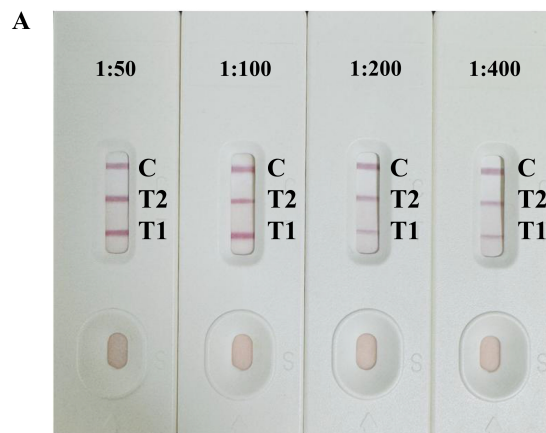


**A**

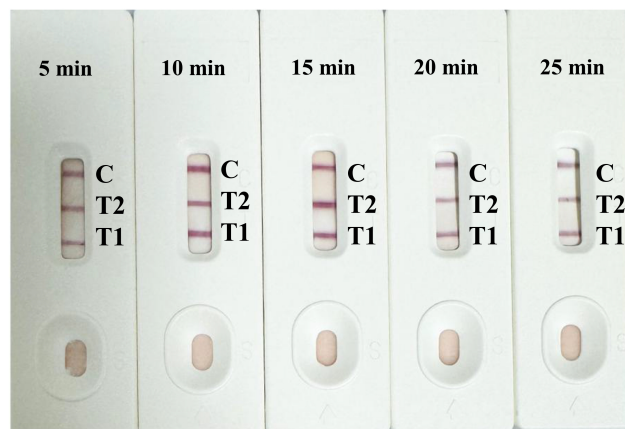


**B**

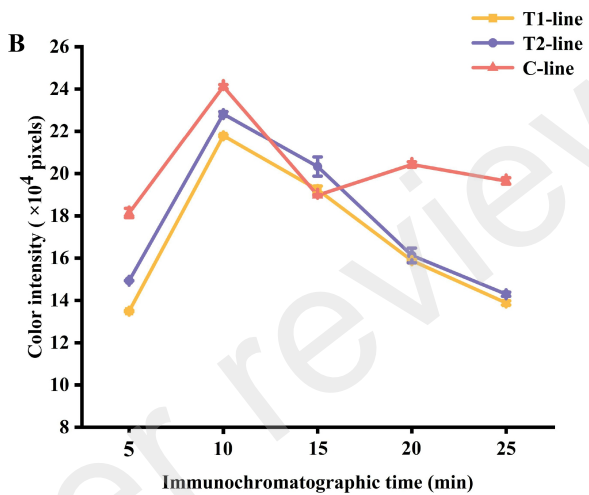




A



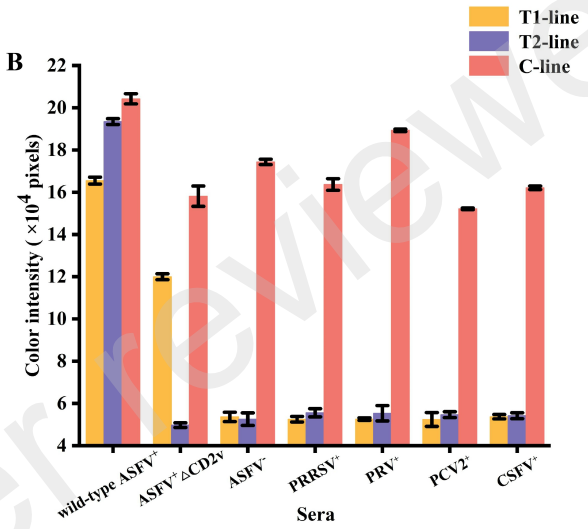
B



A

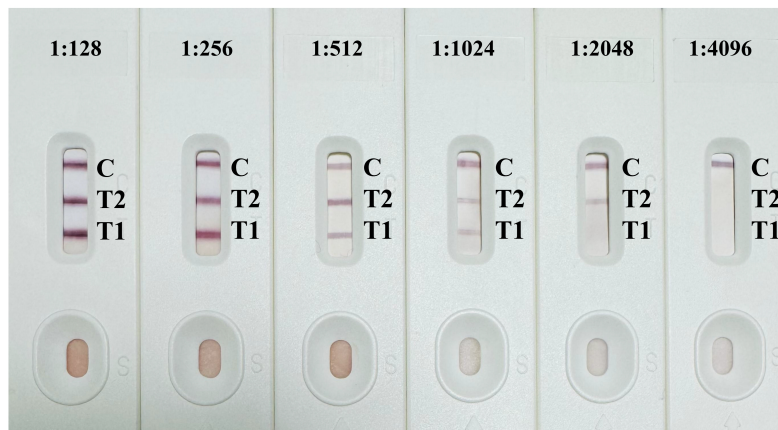


B





A



B

